AJNR Am J Neuroradiol 21:162–170, January 2000

Vascularization of Head and Neck Paragangliomas: Comparison of Three MR Angiographic Techniques with Digital Subtraction Angiography

René van den Berg, Martin N.J.M. Wasser, Adrian P.G. van Gils, Andel G.L. van der Mey, Jo Hermans, and Mark A. van Buchem

BACKGROUND AND PURPOSE: **MR angiography of the head and neck region has been studied widely, but few studies have been performed concerning the efficacy of MR angiography for the identification of the specific vascular supply of the highly vascular head and neck paragangliomas. In this study, we compared three MR angiography techniques with respect to visualization of branch arteries in the neck and identification of tumor feeders in patients with paragangliomas.**

METHODS: **Fourteen patients with 29 paragangliomas were examined at 1.5 T using 3D phase-contrast (PC), 2D time-of-flight (2D TOF), and multi-slab 3D TOF MR angiography. In the first part of the study, two radiologists independently evaluated the visibility of first-, second-, and third-order branch arteries in the neck. In the second part of the study, the number of feeding arteries for every paraganglioma was determined and compared with digital subtraction angiography (DSA), the standard of reference in this study.**

RESULTS: **Three-dimensional TOF angiography was superior to the other MR angiography techniques studied ($P < .05$) for depicting branch arteries of the external carotid artery in the neck, but only first- and second-order vessels were reliably shown. DSA showed a total of 78 feeding arteries in the group of patients with 29 paragangliomas, which was superior to what was revealed by all MR angiography techniques studied. More tumor feeders were identified with 3D TOF and 2D TOF angiography than with 3D PC MR angiography ($P < .05$), with a sensitivity/specificity of 61%/98%, 54%/95%, and 31%/ 95%, respectively. Sensitivity was lowest for carotid body tumors.**

CONCLUSION: **Compared with intra-arterial DSA, the 3D TOF MR angiography technique was superior to 3D PC and 2D TOF MR angiography for identifying the first- and second-order vessels in the neck. With 3D TOF angiography, more tumor feeders were identified than with the other MR angiography techniques studied. The sensitivity of MR angiography, however, is not high enough to reveal important vascularization. The sensitivity of MR angiography is too low to replace DSA, especially in the presence of carotid body tumors.**

Paragangliomas of the head and neck are highly vascular neoplasms that originate from paraganglionic tissue located at the carotid bifurcation (carotid body tumors), along the nodose ganglia of the vagus nerve (vagal paragangliomas), and in the jugular fossa and tympanic cavity (jugulotympanic paragangliomas). Paragangliomas are rarely malignant. In general, they are very slow-growing, benign neoplasms. Paraganglioma-associated morbidity occurs because of local tumor growth compromising neural and vascular structures in the neck, skull base, and posterior cranial fossa. Such morbidity may be an indication for treatment, which comprises surgical resection with or without preceding embolization.

Diagnostic radiology plays an important role in the analysis of a paraganglioma patient. First, the tumor has to be detected and characterized, and because paragangliomas are multiple in 30% of patients, the presence of concomitant tumors also should be studied. In addition, tumor extension has to be determined, especially the relation of the tumor to the surrounding vascular structures. For

Received January 21, 1999; accepted after revision July 12.

From the Departments of Radiology (R.v.d.B., M.N.J.M.W., M.A.v.B.) and Otolaryngology (A.G.L.v.d.M.), Leiden University Medical Center; the Department of Medical Statistics (J.H.), University of Leiden; and the Department of Radiology (A.P.G.v.G.), Utrecht University Hospital, the Netherlands.

Address reprint requests to René van den Berg, Department of Radiology, Bldg 1, C2-S, Leiden University Medical Center, Albinusdreef 2, 2333 AA Leiden, The Netherlands.

these tasks, MR imaging is well equipped and has proved to be superior to other imaging techniques (1–4). Once it has been decided that an operation is indicated, detailed information about the vascular supply of the tumors is required. When information regarding the angioarchitecture of the vascular supply of paragangliomas has been obtained, a therapeutic decision can be determined based on whether such a lesion can be embolized. This also results in a reduction of operative risk. Digital subtraction angiography (DSA) is the diagnostic method of choice for obtaining this vascular information.

MR angiography has several advantages over DSA. The most obvious is its lack of morbidity and mortality. In addition, because of the availability of the source images as well as the possibility of generating maximum-intensity projections (MIPs), spatial relationships between blood vessels and surrounding structures can be assessed optimally. Two previous investigations (5, 6), both studying six patients, demonstrated that identification of feeders of paragangliomas is feasible with MR angiography. Other articles regarding the role of MR angiography for assessment of vascularization of paragangliomas reported unsuccessful attempts at identifying feeding vessels (7, 8).

Systematic studies on the efficacy of MR angiography for identifying tumor feeders in patients with paragangliomas are lacking in the literature. A prerequisite for establishing the utility of MR angiography techniques for identifying tumor feeders is to explore the reliability of this technique for identifying normal branch arteries in the neck. We are not aware of any studies in the literature that explore this aspect of MR angiography. In this study, we attempted to study the efficacy of three MR angiography techniques—3D phase-contrast (PC), 2D time-of-flight (TOF), and 3D TOF angiography—to determine which technique enabled optimal visualization of branch arteries in the neck. We also attempted to study the efficacy of these MR angiography techniques with respect to identification of tumor feeders in patients with paragangliomas.

Methods

Patients

Fourteen patients (seven female, seven male; median age, 39 years [range, 29–57 years]) with 29 paragangliomas were studied. These 29 paragangliomas included 13 carotid body tumors, ten vagal paragangliomas, and six jugulotympanic paragangliomas. Four patients had solitary carotid body tumors. All other patients had multiple paragangliomas: four patients with two, five patients with three, and one patient with four tumors. In this group of 29 paragangliomas, a total of 78 feeding arteries were identified with DSA.

In five patients, DSA was performed within 3 months after MR angiography. In the other nine patients, DSA was performed prior to MR angiography. The interval between DSA and MR angiography ranged from 3 to 22 months (mean, 12 months). None of these patients underwent embolization or surgery in the period between DSA and MR angiography.

MR Angiography Acquisition

MR angiography was performed on a Philips NT 15 gyroscan (Philips Medical Systems, Best, the Netherlands) operating at a field strength of 1.5 T and with a standard quadrature neck coil. The imaging protocol included three axial MR angiography sequences using thin-section gradient-echo pulse sequences covering an area of 10 centimeters from the distal common carotid artery upward. Field of view (200 mm) and matrix size (196 × 256) were identical for all techniques. The scan parameters for 3D PC MR angiography were 26/9/2 (TR/TE/excitations); flip angle, 20°; 50 over-contiguous slices; and slice thickness, 4 mm with 2-mm overlap. A band to suppress venous flow signal was placed cranially to the imaging volume. Scan time was 11 minutes 39 seconds. Both magnitude and phase images were evaluated. In a pilot study, we assessed the optimal velocity encoding for the PC MR angiography technique. Using an encoded velocity of 20 cm/s, we found some signal loss in the carotid bifurcation due to aliasing, but no signal loss in the external carotid artery itself. This velocity encoding value was chosen to optimize visualization of the small feeding arteries. Two-dimensional TOF scan parameters were 28/5.1/2 (TR/TE/excitations); flip angle, 60°; 50 slices; and slice thickness, 2 mm. A travelling band for saturation of venous flow was placed cranially to every slice. The scan time was 4 minutes 17 seconds. A gradient-echo technique with five overlapping slabs was used for 3D TOF MR angiography. Cranial to each separate slab, a saturation band was placed to suppress venous flow. This multi-slab technique reduces the saturation of flow signal. Scan parameters were 25/6.9/1 (TR/TE/excitations); flip angle, 20°; 135 over-contiguous slices; and slice thickness, 1.5 mm with 0.75 mm overlap. The scan time was 5 minutes 49 seconds.

From the individual source images of the three MR angiography data sets, MIPs were generated using the software provided by the manufacturer of the MR system. Nine projections were obtained rotating around the craniocaudal axis at 20° increments. For each case, identical MIPs were generated of each MR angiography sequence. Subregions of interest on the MIPs were only made for illustrative purposes in this investigation; none of them were used during the reading sessions. MIPs and axial source images were evaluated as described in the following section.

MR Angiography Interpretation

For each MR angiography technique, the combined set of axial source images and MIPs were evaluated independently by two radiologists (APGvG, MNJMW). They had no knowledge of the DSA results. Before reviewing the data sets, both readers first were trained to identify the normal vascular anatomy on MR angiography, both in the axial plane as well as on the MIPs. Correct identification of branch arteries in the neck in the axial plane is possible, because the endpoint is fixed, and the origin shows only a small number of variations (9). This is also true in patients with paragangliomas, because only the course of these vessels, and not their origin (or endpoint), is affected by the tumor.

To eliminate the potential effect of a learning curve, the complete set of 3D PC, 2D TOF, and 3D TOF MR angiography studies were randomized before they were presented to the two readers. The order of presentation of the different techniques was, therefore, also random.

The readers were not blinded to the type of technique used because the axial slices of the MR angiograms were so different that hiding the acquisition parameters was not very useful.

The time available for interpreting the images was unrestricted. The reading sessions took place in a period of 3 months.

TABLE 1: Percentage of good visibility* of 39 normal neck arteries as determined by the three different MR angiography techniques for both readers

	Reader 1			Reader 2		
	PCA	2D TOF	3D TOF	PCA	2D TOF	3D TOF
First order (n = 7)						
Internal carotid a.	100	100	100	100	100	100
External carotid a.	100	100	100	100	100	100
Vertebral a.	100	100	100	96	100	100
Basilar a.	89	100	100	68	100	100
Average	97.3	100	100	91.0	100	100
Second order (n = 20)						
Superior thyroid a.	68	73	68	46	43	69
Lingual a.	36	42	46	32	44	46
Facial a.	54	71	79	57	50	79
Ascending pharyngeal a.	57	83	93	50	75	89
Occipital a.	79	87	96	61	86	100
Posterior auricular a.	32	27	48	4	4	15
Superficial temporal a.	75	96	100	61	91	100
Maxillary a.	75	100	100	82	100	89
PICA	43	59	83	21	57	40
AICA	22	28	50	35	42	83
Average	54	66	76	45	59	71
Third order (n = 12)						
Ascending palatine a.	11	38	7	21	25	18
Occipital branches	50	29	50	21	21	39
Meningeal a.	43	82	89	39	82	65
Masseteric a.	18	27	20	29	33	22
Deep temporal a.	8	32	27	4	6	17
Deep auricular a.	15	0	27	4	5	0
Average	24	34	36	20	28	26
Total Friedman ranking	28	42	50†	28	44	48†

Note.—a. = artery, PICA = posterior inferior cerebellar artery, AICA = anterior inferior cerebellar artery.

* Good visibility means visibility of the complete course of the vessel.

† Friedman test $P < .05$ for both readers.

Image Quality

The readers were asked to assess the quality of the axial source images in terms of: 1) tumor visibility, 2) presence of ghost artifacts from pulsatility of vessels, and 3) degree of saturation of venous flow. Tumor visibility was rated as ''good'' when the margins of the tumor and the tumor itself were well defined. It was rated ''moderate'' when only the tumor was visible, but the margins could not be defined clearly. Tumor visibility was ''poor'' when only indirect signs of a mass were noticed, such as displacement of the internal and external carotid arteries.

Identification of Branch Arteries

We defined the internal, external, vertebral, and basilar artery as first-order vessels (n=7). External carotid artery branches, posterior inferior cerebellar artery (PICA), and anterior inferior cerebellar artery (AICA) were defined as second-order vessels (n=20). Branches of each of the second-order vessels were defined as third-order vessels (n=12). The visibility of these 39 arteries was assessed in each MR angiography study. Detailed information on the identity of the neck arteries is shown in Table 1. The readers graded the visibility of each artery on a four-point scale. Visibility of the complete course of the vessel was rated as ''good,'' visibility of only the proximal part of the vessel was rated as ''moderate,'' visibility of only the origin of the vessel was rated as ''poor,'' and, finally, the vessel could be rated as ''not visible.''

Identification of Tumor Feeders

The number of feeding arteries for each paraganglioma was assessed for each of the three MR angiography techniques. With MR angiography, no direct evidence is present that a vessel is really supplying the tumor, because no tumor opacification is seen. We considered a vessel a feeder when it entered the tumor and lost its flow signal on the consecutive slices in the tumor.

For each feeding artery, the readers were asked to give their degree of confidence using a five-point scale: 1) definitely present, 2) probably present, 3) equivocal, 4) probably absent, and 5) definitely absent. Very small (< 0.5 mm) branches from the external carotid artery supplying the vascular envelope of the carotid body tumors were not included in the analysis as feeders, because they are of minor importance during surgery.

Paragangliomas not only receive their blood supply from the carotid and vertebral arteries, but they can also be vascularized by the deep cervical artery and thyrocervical trunk. In this study, these vessels were only visualized in one patient in whom an aortic arch angiogram was obtained. Therefore, a standard of reference based on the combined set of MR angiograms was made by the study coordinator to compare the detection rate of these two vessels for the three MR angiography techniques. The results for the detection of these vessels were not used in the statistical analysis to calculate sensitivity and specificity.

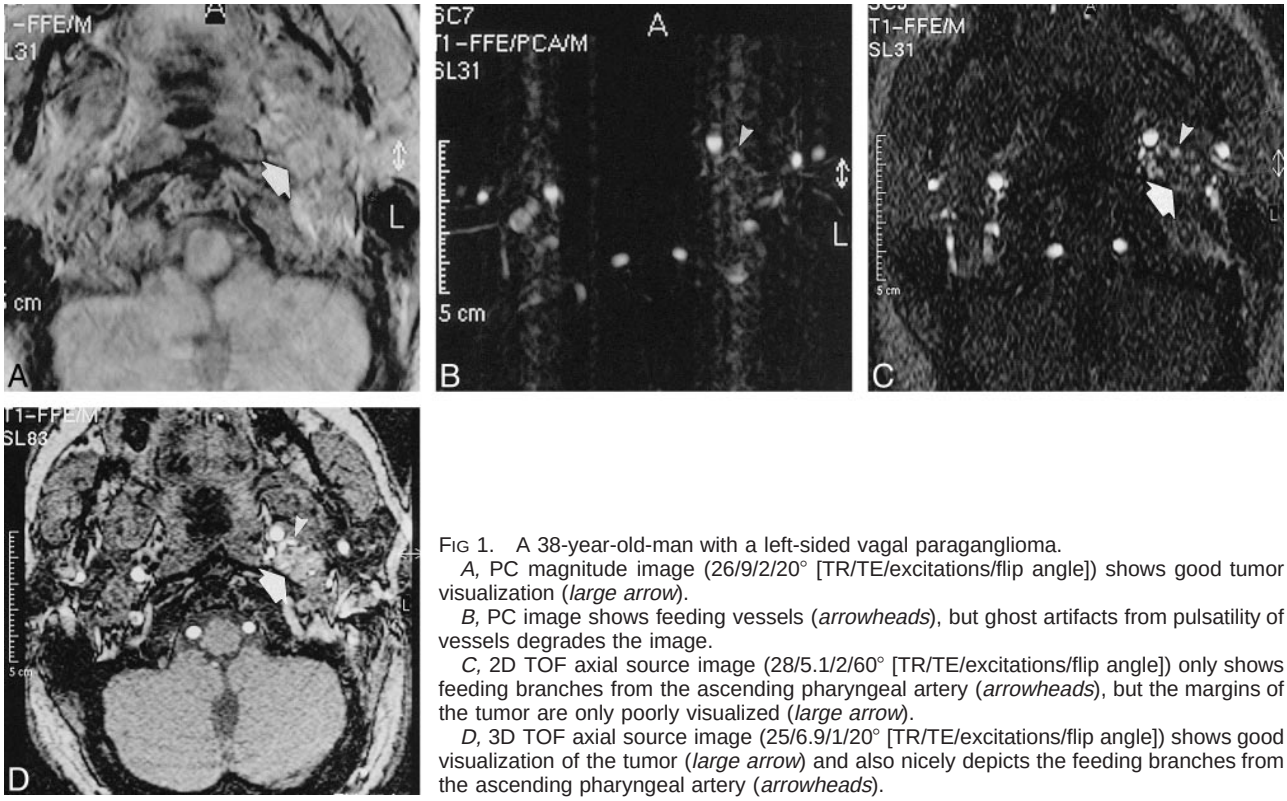

FIG 1. A 38-year-old-man with a left-sided vagal paraganglioma.

A, PC magnitude image (26/9/2/20° [TR/TE/excitations/flip angle]) shows good tumor visualization (*large arrow*).

B, PC image shows feeding vessels (*arrowheads*), but ghost artifacts from pulsatility of vessels degrades the image.

C, 2D TOF axial source image (28/5.1/2/60° [TR/TE/excitations/flip angle]) only shows feeding branches from the ascending pharyngeal artery (*arrowheads*), but the margins of the tumor are only poorly visualized (*large arrow*).

D, 3D TOF axial source image (25/6.9/1/20° [TR/TE/excitations/flip angle]) shows good visualization of the tumor (*large arrow*) and also nicely depicts the feeding branches from the ascending pharyngeal artery (*arrowheads*).

Digital Subtraction Angiography

DSA was performed in all patients with selective injection of the common carotid, external carotid, and vertebral arteries. All images were obtained in anteroposterior and lateral directions. An aortic arch angiogram was not performed routinely. The DSA studies were evaluated independently by a radiologist experienced in DSA (RvdB), who identified tumor feeders in each case.

Statistical Analysis

First, we determined which of the three MR angiography techniques was best for visualizing branch arteries of the neck. The number of times, summed for all 14 patients, that an artery showed ''good'' visibility was converted into a percentage. The Friedman test (10) was used to demonstrate differences between the three techniques. The three percentages for the three MR angiography techniques were ranked per reader and per artery. The difference in percentage for the visibility between the MR angiography techniques had to be more than 5% to give it a different ranking. The best, intermediate, and poorest technique received three, two, and one point(s), respectively, in this ranking. When no differences were found, points were divided equally. The best technique has the highest total ranking for all arteries.

Second, we determined the potential of the three MR angiography techniques for identifying the presence of feeding arteries of paragangliomas. The results were subjected to receiver operating characteristic (ROC) analysis. From these data, the area under the ROC curve was calculated for each technique and each reader. For comparison of these areas under the curve, the *z*-test was used, with $P < .05$ as the level of significance. To determine sensitivity and specificity, the results were divided by putting the threshold between probably and equivocally present scores.

Finally, the interobserver agreement of the different MR angiography techniques for both study parts was determined. This was done by calculating kappa values (κ) and by determining how often the readers agreed on 1) grading visibility of the normal vascular anatomy as good and (2) on detecting a feeding artery as definitely or probably present.

Results

Image Quality

Tumor visibility was graded as good in 57%, moderate in 21%, and poor in 22 % for 3D PC studies versus 0% good, 7% moderate, and 93% poor grades for 2D TOF studies and 50% good, 43% moderate, and 7% poor rankings for 3D TOF studies. Examples of these axial source images are shown in Figure 1 for all three MR angiography techniques. Ghost artifacts from pulsatility of vessels deteriorated 3D PC studies in 100% of cases, but in only 14% of those studied with 2D TOF, and in 7% of those studied with 3D TOF MR angiography. Incomplete saturation of venous flow was another major drawback of 3D PC MR angiography, and was present in all cases. With the other two techniques, incomplete saturation was not seen.

Identification of Branch Arteries

Results of visibility of first-, second-, and third-order vessels are shown in Table 1. All first-order vessels showed good visibility with 2D TOF and 3D TOF MR angiography. First-order vessels were moderately visible with 3D PC MR angiography in 3% of cases for reader 1 and in 9% of cases for reader 2. Visibility of second-order vessels was best with 3D TOF compared with the other two

TABLE 2: Number of feeding arteries as detected by the three different MR angiography techniques for both readers as compared with DSA, the standard of reference. Results were divided by putting the threshold between probably and equivocally present rankings.

		Reader 1			Reader 2		
	DSA	PCA	2DTOF	3DTOF	PCA	2DTOF	3DTOF
Ascending pharyngeal a.	24	10	19	17	13	20	18
Occipital a.	21	7	15	13	7	10	11
Unspecified branch ECA	16	3	4	8	8	10	10
Posterior auricular a.	4	0	0	1	0	0	0
Maxillary a.	1	0	1	0	0	0	1
Branch internal carotid a.	2	0	0	0	1	1	2
Muscular branch vertebral a.	5	0	2	5	0	1	3
AICA	2	0	1	1	0	0	2
PICA	3	0	0	2	0	1	3
Total	78	20	42	47	29	43	50
	MRA*	PCA	2DTOF	3DTOF	PCA	2DTOF	3DTOF
Deep cervical a.	1	1	1	1	1	1	1
Thyrocervical trunk†	8	2	4	6	5	6	7

Note.—a. = artery, ECA = external carotid artery, musc. = muscular, AICA = anterior inferior cerebellar artery, PICA = posterior inferior cerebellar artery.

* As determined by the independent study coordinator.

† Aortic arch angiogram performed in one patient confirmed vascularization.

MR angiography techniques. The ascending pharyngeal, occipital, maxillary, and superficial temporal artery showed good visibility in more than 90% of cases (mean for both readers). Of the second-order vessels, the posterior auricular artery showed good visibility in less than 50% of cases. Third-order vessels showed good visibility in 32% of cases with both 2D TOF and 3D TOF techniques and in 22% cases with 3D PC angiography. The meningeal artery, the largest branch of the maxillary artery, was the most visible third-order vessel. Three-dimensional TOF received the highest total ranking with respect to visualization of vessels (Friedman test, $P < .05$) from both readers and for the total group of arteries. It is superior to the other two MR angiography techniques for visualization of the first-, second- and third-order arteries.

Results recorded by both readers were compared to determine the interobserver agreement by using cross tables and kappa values. Using the four-point scale for visibility ranking, a higher degree of agreement was obtained for vessels that were assigned ''good visibility'' with 3D TOF (51%) than with 3D PC (34%) and 2D TOF (44%) MR angiography. For all techniques, the kappa values were low. A slightly better agreement was seen with 2D TOF ($\kappa = 0.32$) and 3D TOF ($\kappa = 0.31$) than with 3D PC ($\kappa = 0.25$) studies.

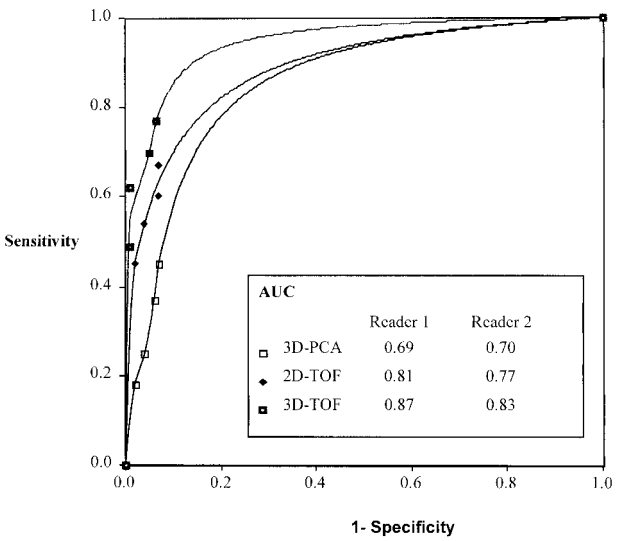

FIG 2. Graph of ROC curves of reader 1 for the three MR angiography techniques shows the highest area under the curve for 3D TOF MR angiography. Areas under the curves (AUC) for both readers are given.

Identification of Tumor Feeders

The results of the detection of feeding arteries for the different MR angiography techniques were compared with DSA for both readers separately (Table 2). ROC analysis showed that, for both readers, the area under the curve was highest for the 3D TOF technique (Fig 2). PC MR angiography was the least sensitive technique ($P < .05$). The difference between 3D TOF and 2D TOF was statistically not significant, but both readers did detect more feeders with 3D TOF MR angiography. Sensitivity of the three MR angiography techniques for tumor feeders also was calculated by tumor localization (Table 3). Sensitivity for the detection of feeding arteries was highest in jugulotympanic paragangliomas compared with carotid body tumors and vagal paragangliomas. This difference in sensitivity was seen with all MR angiography techniques.

When evaluating individual feeding arteries with 3D TOF MR angiography, both readers identified the ascending pharyngeal artery (in five of 10

TABLE 3: Sensitivity percentage for detection of feeding arteries per tumor localization for reader 1 and 2. Results were divided by putting the threshold between probably and equivocally present rankings.

	Reader 1			Reader 2		
	3D PCA	2D TOF	3D TOF	3D PCA	2D TOF	3D TOF
Carotid body tumor	14	49	49	26	54	51
Vagal paraganglioma	23	69	62	23	46	62
Jugulotympanic paraganglioma	36	54	74	59	64	82
All localizations*	25/95	53/96	59/98	37/96	54/94	63/98

* Sensitivity and specificity for all tumor localizations.

FIG 3. A 38-year-old-man with a left-sided vagal paraganglioma. Slightly anteroposterior, oblique MIPs are presented. A muscular branch from the vertebral artery adds to the extensive vascularization of this tumor.

A, 3D PCA MIP (26/9/2/20° [TR/TE/excitations/flip angle]) hardly shows a branch from the occipital artery (*arrow*) as tumor feeder. The muscular branch from the vertebral artery is not at all visible.

B, 2D TOF MIP (28/5.1/2/60° [TR/TE/excitations/flip angle]) not only shows supply from the occipital artery (*arrow*), but a small feeding branch from the vertebral artery (*arrowhead*) also is depicted.

C, 3D TOF MIP (25/6.9/1/20° [TR/TE/excitations/flip angle]) shows more clearly than the 2D TOF MIP vascularization from the occipital artery (*arrow*) as well as from the vertebral artery (*arrowhead*).

cases) and the occipital artery (in four of eight cases) as feeders of carotid body tumors. Two-dimensional TOF technique showed more of these feeders in eight of ten and seven of eight cases. Feeding branches from the vertebral artery were found in tumors localized in the region of the skull base. With the 3D TOF technique, reader 1 identified all tumor supply of the muscular branches from the vertebral artery, two of three PICAs, and one AICA. Reader 2 identified all PICAs and AICAs, but only three muscular branches. Using 2D TOF, only two muscular branches and one AICA and PICA were identified as feeders. None of these feeders were identified with 3D PC angiography (Fig 3).

Using all three techniques, reader 1 did not detect feeders originating from the internal carotid artery. Reader 2 correctly identified vascularization by the internal carotid artery by using PC and 2D TOF techniques in one of two cases and in both cases by using the 3D TOF technique.

The thyrocervical trunk vascularized four carotid body and four vagal paragangliomas. Both readers identified vascularization from the thyrocervical trunk in six and seven of eight cases, respectively, by using the 3D TOF technique (Fig 4). Results were two and five of eight cases identified with PC MR angiography, and four and six of eight cases identified with the 2D TOF technique. In a patient with a large vagal paraganglioma, the deep cervical artery was identified with all three techniques as a major feeder.

Cross-table analysis showed best interobserver agreement for the definite or probable detection of feeding arteries revealed with the 3D TOF technique (49%) compared with that of 3D PC (18%) and 2D TOF (44%) techniques. For all techniques, the kappa values were low. Using the five-point scale for the detection of feeding arteries, a better agreement was seen with 2D TOF ($\kappa = 0.31$) and 3D TOF ($\kappa = 0.31$) than with the 3D PC ($\kappa = 0.23$) technique.

Discussion

The goal of this study was to evaluate the efficacy of MR angiography techniques for identifying tumor feeders in paragangliomas. To our knowledge, this is the first study in which 3D PC, 2D TOF, and 3D TOF MR angiography were correlated systematically with DSA. In order to identify tumor feeders, it is required that the vessels that may sup-

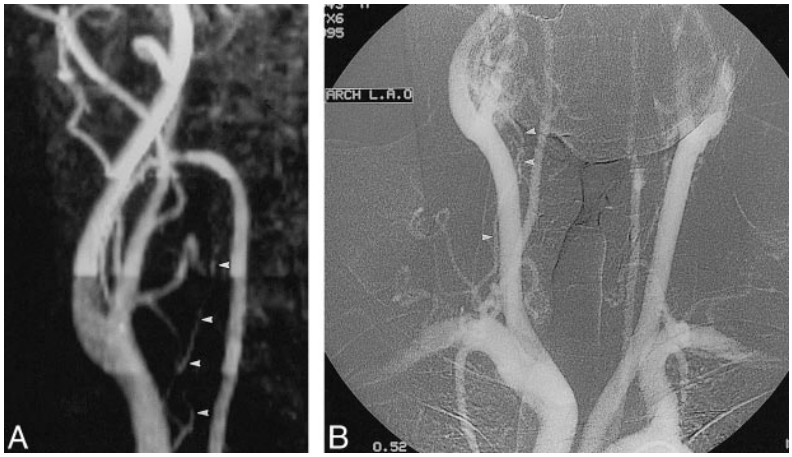

FIG 4. A 53-year-old-man with bilateral carotid body tumors.

A, Anteroposterior view of the 3D TOF MIP (25/6.9/1/20° [TR/TE/excitations/flip angle]) shows the thyrocervical trunk (*arrowheads*), adding to the vascularization of the carotid body tumor.

B, On the aortic arch angiogram, showing both carotid body tumors, the vascularization from the thyrocervical trunk (*arrowheads*) was confirmed.

ply paragangliomas (ie, the branch arteries in the neck) are identifiable using MR angiography sequences. For identification of vessels, one can use axial source images as well as MIPs. The MIP shows excellent contrast as long as the vessel intensity is well above the mean background noise. One of the shortcomings of MIPs is their less intense depiction of the edges versus the centers of vessels. These edges are the first to be obscured by background fluctuations. Because of this, vessels appear narrower than on individual sections (11). Smaller vessels, such as the branch arteries, can even disappear on the MIP. Because of the reduced depiction of the arteries on MIPs, Blatter and colleagues (12) used axial source images specifically to identify the branch arteries. Identification of branch arteries of the external carotid artery on axial images is possible, because the origin shows only a small number of variations (9). From its origin, the vessel can be followed on the consecutive slices toward its territory, which unequivocally determines the identity of the vessel.

In the first part of this study, we compared three MR angiography techniques with respect to identification of the branch arteries of the external carotid artery. The results showed a statistically significant better performance for 3D TOF MR angiography compared with 3D PC and 2D TOF MR angiography. This better performance can be explained by the superior spatial resolution and the difference in slice thickness of the 3D TOF technique (1.5 mm), the latter of which influences voxel size (13), as compared with the slice thicknesses of 3D PC (4 mm) and 2D TOF (2 mm) techniques. Difference in slice thickness was chosen because, with 3D PC MR angiography, 2-mm slices would have resulted in a scan time of 23 minutes and, with 2D TOF technique, a slice thickness below 2 mm would have caused a significant drop in the signal-to-noise ratio. Because matrix and field of view were equal for all techniques, voxel size was defined by the slice thickness. Voxel size relative to the diameter of the vessel determines whether a vessel can be depicted or not. Against the advantageous slice thickness of 3D TOF are theoretical advantages of 3D PC technique, including background suppression, minimized saturation effects, and variable velocity encoding. Advantages of 2D TOF are its sensitivity to slow flow and lack of saturation effects (13). Saturation, secondary to prolonged in-plane flow, should only be expected in horizontally oriented vessels—ie, the lingual and facial artery. These vessels, however, were not depicted better using 2D TOF and 3D PC than with 3D TOF MR angiography. The finding that vessel detail was not seriously degraded on the axial images also has been observed in a previous report (12). The theoretical advantages of 3D PC and 2D TOF MR angiography with respect to saturation effects did not compensate for the disadvantage of the slice thickness. Our results showed that, when using the best MR angiography technique (3D TOF), a rating of good visibility of first-, second-, and third-order vessels was assigned to 100%, 75%, and 50% of cases, respectively. Visualization of the third-order vessels only occurred in 50% of cases, which is very low, and can be explained by the size of these vessels relative to the voxel size, which makes visualization of these smaller vessels very difficult. Three-dimensional TOF MR angiography is, therefore, only suitable for identification of the first-order (internal and external carotid and vertebral artery) and second-order (branch arteries of the external carotid artery) vessels in the neck.

In the second part of the study, we determined the efficacy of the three MR angiography techniques with respect to identification of tumor feeders. Findings were correlated with DSA, which served as the standard of reference. MR angiography has the advantage over DSA in that it can display vascular structures in the axial plane without superimposition. Mean sensitivity/specificity for both readers for all tumor localizations were: PC, 31%/96%; 2D TOF, 54%/95%; and 3D TOF, 61%/98%. Differences between 2D TOF and 3D TOF were statistically not significant, but both readers did identify more feeders with 3D TOF imaging. The fact that we did not reach a statistically significant difference is probably related to the

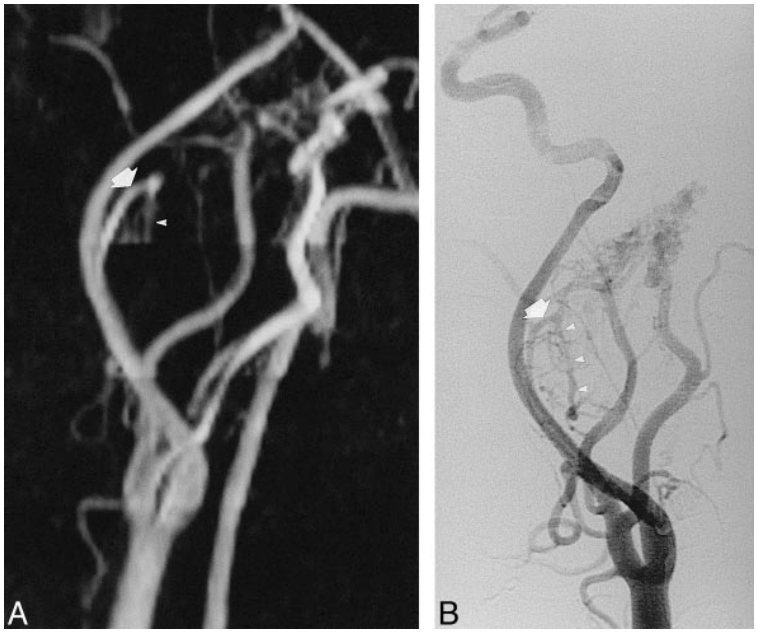

FIG 5. A 49-year-old-man with a vagal paraganglioma (*lateral view*).

A, 3D TOF MIP (25/6.9/1/20° [TR/TE/excitations/flip angle]) shows enlarged ascending pharyngeal artery (*large arrow*) as a feeder despite the fact that the cranially placed slab for saturation of venous flow obscures the descending trunk of this artery (*arrowheads*).

B, On the digital subtraction angiogram, the complete course of the ascending pharyngeal artery (*large arrow*), including its descending trunk (*arrowheads*), is visible.

small number of patients in this study. These results follow the same trend as what was found with the identification of branch arteries, and again can be explained by the voxel size used.

Remarkable differences in detection rate were seen when tumor localization was taken into account. Detection of feeding arteries was better in jugulotympanic paragangliomas as compared with carotid body tumors and vagal paragangliomas. This can be explained by the course of the feeding arteries. Jugulotympanic paragangliomas are supplied by vessels following a caudocranial course that is not prone to saturation, secondary to prolonged in-plane flow. In carotid body tumors and vagal paragangliomas, the occipital and ascending pharyngeal arteries are the most frequent feeders that often have to make a loop to supply the tumor. Visualization of the entire loop is especially limited with 3D TOF MR angiography because, with this multi-slab technique, a saturation band is applied cranially to each slab to suppress venous blood flow in the craniocaudal direction. When 3D TOF MR angiography is used, and the vessel loop traverses two slabs, the saturation band suppresses the part of the loop in the more caudal slab (Fig 5). Because of this technical limitation, the ascending pharyngeal and occipital arteries were identified as feeders in carotid body tumors in only nine of 18 cases when using 3D TOF MR angiography. The loss of signal in the loop was less pronounced with 2D TOF than with 3D TOF MR angiography. With 2D TOF, the ascending pharyngeal and occipital artery were identified correctly as feeders of carotid body tumors in 15 of 18 cases. Elimination of this loop effect when using 3D TOF technique is only possible by removing the saturation band, but this makes the differentiation between arteries and veins more difficult. The result would be an increase in sensitivity, but only at the cost of specificity.

Our results show that, with the current MR angiography techniques, MR angiography is not sufficient for identifying specific feeding vessels supplying paragangliomas. The sole purpose of patients with carotid body tumors undergoing intra-arterial angiography is to inform the surgeon of specific vascular supply. Preoperative embolization is seldom necessary for this tumor localization. Therefore, these patients would benefit most from a noninvasive angiographic study, such as MR angiography, to show the specific feeding vessels. Unfortunately, the sensitivity of 3D TOF MR angiography for showing these feeding vessels is too low to replace DSA. Because preoperative embolization is almost always performed in patients with vagal and jugulotympanic paragangliomas, one can argue for performing MR angiography. The only reason to perform MR angiography would be to exclude the presence of feeding vessels that can be embolized. Then, an intra-arterial angiography, in combination with an embolization, can be prevented. Sensitivity to visualizing feeding vessels, however, is also too low for vagal and jugulotympanic paragangliomas, and even the best MR angiography technique cannot reliably exclude the presence of vessels that can be embolized. Therefore, for all three tumor localizations, DSA cannot be replaced by MR angiography.

It remains to be studied whether contrast-enhanced MR angiography will be able to show more feeding vessels than the three MR techniques evaluated in this study. One of the problems that can be expected with the contrast-enhanced technique is the very rapid arteriovenous transit of contrast in these highly vascular lesions. This results in very early enhancement of the venous structures, masking the visualization of the arterial system. Furthermore, the slice thickness of this technique is, at

the moment, too large to make visualization of the smaller vessels possible.

This study has some shortcomings. The 1-year mean interval between DSA and MR angiography is rather long. These highly vascular lesions have a slow but continuous growth rate (14). Therefore, patients were included only after confirmation by MR imaging that the tumor size had not changed in the period between DSA and MR angiography. The presumption was made that if tumor size did not change over a longer period of time, the number of feeding arteries would not change dramatically. If new feeding arteries arose during this interval, all three MR angiography techniques would have yielded false-positive findings, resulting in a lower specificity. Therefore, the interval is only a relative weakness in the study design that would not affect the results of the comparison of the three MR angiography techniques.

The requirement to identify the branch arteries in the axial plane is another shortcoming. The readers were trained to identify carefully the vascular anatomy in the axial plane. Despite this training, session misregistrations occurred. Only one of the two readers identified important feeding vessels from the internal carotid and vertebral artery. This means that 3D TOF MR angiography depicted all feeders from the internal carotid artery, AICA, PICA, and muscular branches of the vertebral system. The complementary results for both readers regarding identification of tumor feeders shows that, in this study, they are a limiting factor. The assessment of vascularization in the axial plane is too reader-dependent to make it a useful tool for routine clinical practice. This partially explains the low interobserver agreement in this study. This low interobserver agreement also is caused by the semiquantitative study design for both parts of the study, because the readers were asked to give their degree of confidence by using a four- and five-point scale, respectively. Kappa values only display whether there is complete agreement or not, and they do not take into account the magnitude of difference, as given in the confidence levels. This will have a negative effect on the interobserver agreement because relatively small differences in interpretation of the MR angiograms will be judged as completely different readings reflected in the kappa value. Therefore, we also assessed how often the readers agreed in grading visibility of the normal vascular anatomy as good, and in detection of a feeding artery as definitely or probably present. These data showed a 50% agreement for the two readers, which is still not very high. The major determinant for the low kappa value is, therefore, the misregistration of the branch arteries in the neck, as explained previously.

In summary, the multi-slab 3D TOF technique is superior to 3D PC and 2D TOF MR angiography for identification of the first- and second-order vessels in the neck. Most tumor feeders also were identified when using 3D TOF MR angiography. Sensitivity of 3D TOF MR angiography, however, is too low to show the specific feeding vessels in head and neck paragangliomas and, therefore, it cannot replace DSA.

References

1. Olsen WL, Dillon WP, Kelly WM, Norman D, Brant-Zawadski M, Newton TH. **MR imaging of paragangliomas.** *AJR Am J Roentgenol* 1987;148:201–204
2. Phelps PD, Cheeseman AD. **Imaging jugulotympanic glomus tumors.** *Arch Otolaryngol Head Neck Surg* 1990;116:940–945
3. Vogl TJ, Brüning R, Schedel H, et al. **Paragangliomas of the jugular bulb and carotid body: MR imaging with short sequences and Gd-DTPA enhancement.** *AJNR Am J Neuroradiol* 1989;10:823–827
4. Van Gils APG, Van den Berg R, Falke THM, et al. **MR diagnosis of paraganglioma of the head and neck: value of contrast enhancement.** *AJR Am J Roentgenol* 1994;162:147–153
5. Vogl TJ, Juergens M, Balzer JO, et al. **Glomus tumors of the skull base: combined use of MR angiography and spin-echo imaging.** *Radiology* 1994;192:103–110
6. Endres D, Manaligod J, Simonson T, McCulloch T, Hoffman H. **The role of magnetic resonance angiography in head and neck surgery.** *Laryngoscope* 1995;105:1069–1076
7. Win T, Lewin JS. **Imaging characteristics of carotid body tumors.** *Am J Otolaryngol* 1995;16:325–328
8. Rippe DJ, Grist TM. **Carotid body tumor: flow sensitive pulse sequences and MR angiography.** *J Comput Assist Tomogr* 1989; 13:874–877
9. Von Lanz T, Wachsmuth W. **Arteriën des kopfes.** In: Lang J, ed. ***Praktische Anatomie, Kopf (teil A).*** Berlin Heidelberg New York: Springer Verlag;1985:539–560
10. Petrie A. ***Lecture Notes on Medical Statistics.*** Oxford: Blackwell Scientific Publication;1990:171–186
11. Anderson CM, Saloner D. **Artifacts in maximum-intensity-projection display of MR angiograms.** *AJR Am J Roentgenol* 1990; 154:623–629
12. Blatter DD, Parker DL, Robinson RO. **Cerebral MR angiography with multiple overlapping thin slab acquisition. Part I: quantitative analysis of vessel visibility.** *Radiology* 1992;179: 805–811
13. Huston III J, Ehman RL. **Comparison of time-of flight and phase-contrast MR neuroangiographic techniques.** *Radiographics* 1993;13:5–19
14. Gulya AJ. **The glomus tumor and its biology.** *Laryngoscope* 1993;103:7–15